*Progress In Electromagnetics Research B, Vol. 14, 87–106, 2009*

# DIVERSITY MONOPULSE ANTENNA BASED ON A DUAL-FREQUENCY AND DUAL MODE CRLH RAT-RACE COUPLER

**D. de Castro Galán, L. E. García Muñoz and D. Segovia Vargas**

Dpto. Teora de la Señal y Comunicaciones
U. Carlos III de Madrid
Avda. Universidad 30, Leganes, Madrid 28911, Spain

**V. González Posadas**

Dpto. Ing. Audiovisual y Comunicaciones,
U. Politécnica de Madrid
Ctra. Valencia km 7, Madrid 28031, Spain

**Abstract**—A diversity monopulse antenna is presented in this paper. This monopulse antenna is based on a dual frequency dual mode rat-race coupler that has been designed by using Composite Right/Left Handed (CRLH) Transmission Lines (TL). The device has two input ports while the ($\Sigma$) and ($\Delta$) outputs are interchangable at either of the two operating frequencies. In this way the monopulse antenna can work at two different frequencies with two sets of radiation patterns, $\Sigma$ and $\Delta$. In addition, there is no need of diplexing to separate the ($\Sigma$) and ($\Delta$) radiation patterns since these patterns at either frequency are directly obtained at different ports. The dual frequency dual mode rat-race requires that the phase delay of the CRLH lines must be different at either working frequency. As an example of an application, a 950 MHz/1.8 GHz dual-band dual-mode rat-race coupler is shown.

## 1. INTRODUCTION

Direction of Arrival (DoA) systems are based on antenna arrays that optimize a function to obtain the corresponding direction of arrival from any source [1]. One of the earliest tracking systems is the well-known monopulse antenna in which two radiating elements provide,

Corresponding author: D. Segovia Vargas (dani@tsc.uc3m.es).

by means of a microwave circuit, two different radiation patterns, sum ($\Sigma$) and difference ($\Delta$). The amplitude and the phase of the difference output can be used as an indicator of the source angle of arrival (AoA), while the sum output is used as a normal communication link. Propagation problems such as multipath or radar clutter can cause the DoA system to fail. For that reason any diversity techniques included in the monopulse antenna is always to be welcomed since it can help to overcome the previous problem making the system more robust. Besides, it would be desirable to achieve these improvements without greatly increasing the complexity of the proposed monopulse antenna. Frequency diversity techniques are proposed to be included in the monopulse antenna to increase its performance. Then, with this additional diversity, a reduction in the DoA estimation error in the near broadside situation can be achieved because of the sharper slope of the difference radiation pattern at the upper frequency.

Monopulse antennas [2, 3] are based on the 180° rat-race hybrid that can provide the ($\Sigma$) and ($\Delta$) outputs. The inclusion of diversity techniques [4] in the monopulse antenna without increasing its complexity implies substituting directly the hybrid by another device that can help to achieve the proposed diversity techniques.

Frequency diversity can be achieved by using a dual frequency rat-race. Several techniques have been used to achieve dual frequency in hybrid devices. For example, in [5] the use of CRLH lines is proposed to achieve arbitrary dual band components [17]. In [6], the use of open or short circuited stubs is proposed to achieve a dual frequency branch-line. This last approach is not valid for the monopulse antenna since the ($\Sigma$) and ($\Delta$) outputs are needed. If the dual frequency rat-race were substituted by a dual-frequency that could interchange the ($\Sigma$) and ($\Delta$) outputs at the two working frequencies, then the diversity monopulse system could be achieved.

The use of CRLH lines opens new possibilities for multifrequency and miniaturized circuits [7]. CRLH lines and metamaterials are being thoroughly studied nowadays due to the fact that they provide properties not found in common materials [8–12]. Usually, these metamaterials are composed of a periodic arrangement of an electrically small cell in 1, 2 or 3 dimensions [9]. As the unit cell is much smaller than the wavelength, the structure behaves as if it were a uniform medium, which can be characterized by an equivalent negative permittivity ($\epsilon$) and permeability ($\mu$) resulting in an anti-parallel phase and group velocities (the phase propagates backwards with respect to the energy).

This property of the LH and CRLH TLs makes new designs possible for many microwave circuits [13, 14] and antennas [15, 16].

Furthermore, size reduction and bandwidth improvement has been obtained in 180° hybrids by replacing the 270° RH line with a −90° LH line [13], high coupling has been achieved in couplers [14] and dual-frequency branch line or rat-race hybrids [5] by replacing the conventional 90° RH lines with CRLH TLs to obtain the same delays at two different frequencies. Previous circuits have made use of the fact that CRLH lines can present the same phase delay at two different frequencies. A further step could be taken by exploiting the fact that the phase delay at two different frequencies can be arbitrarily controlled (not necessarily the same phase delay but different phase delays for the same line). A first approach for this approach was taken in [18] where a compact diplexer was by making use of CRLH lines.

In this paper CRLH TLs with arbitrary phase delays are used to achieve a dual frequency dual mode rat-race. This allows having a dual frequency dual mode rat-race where the input ports are fixed and connected to two radiating elements while the output ports provide the ($\Sigma$) and ($\Delta$) functions alternatively at both working frequencies. In this way, the monopulse function is directly achieved without any external diplexers.

The paper is organized as follows. Section 2 describes the architecture and fundamental characteristics of the proposed dual-band dual-mode Rat-Race (DBDMRR). Section 3 presents the analysis and design of the CRLH TL. Section 4 presents the simulations and measurements of the proposed device and Section 5 shows the performance of the monopulse antenna. Finally, Section 6 gives the conclusions.

## 2. DUAL-BAND DUAL-MODE RAT-RACE COUPLER: DESIGN

The conventional rat race is composed of three $\lambda/4$ lines and one $3\lambda/4$ line (Figure 2(a)). If port 1 is taken as an input port, the signal will be evenly split into two in-phase signals at ports 2 and 4, while port 3 will be isolated. The same result will be obtained if the input port is the port 4 resulting in two 180 out of phase output ports (1 and 3) while the port 2 is the isolated one. As is well known, the circuit can also work as a combiner: if two signals are applied to ports 2 and 4, the sum ($\Sigma$) will appear at port 1 while the difference ($\Delta$) will be at port 3. The proposed topology for the diversity monopulse antenna would require two different conventional rat-race couplers at the same time. This can be seen in Figure 5.b where the two antennas working at $f_1$ and $f_2$ are connected at the input ports (named 2 and 4) of two different rat-race couplers working at $f_1$ and $f_2$. The overall monopulse system would

require then an external diplexer to separate the different output ports, ($\Sigma$) and ($\Delta$), at either frequency. This would result in increasing the complexity of the monopulse antenna. The complexity of the proposed monopulse system is reduced by making use of CRLH lines that can have two different phase delays at the proposed working frequencies. In that case, the new compact topology for the diversity monopulse antenna is shown in Figure 2 where the position of the antennas has been kept unchanged with respect to Figure 1(b) and the electrical lengths of the lines have been changed to obtain the desired behavior. Thus, three different lines must be designed: two dual frequency TLs of $-90°/-90°$ one dual frequency TL with a phase shift $-90°/90°$ and other dual frequency TL with a phase shift of $90°/-90°$ at $f_1$ and $f_2$, respectively. This is summarized in Table 1. The schematic of the propose d device (Figure 2) shows two sets of electrical lengths: the inner part of the hybrid corresponds at one frequency while the outer part at the other.

**Table 1.** Electrical length for the three lines.

| | $f_1$ | $f_2$ |
|---|---|---|
| $\phi_{C\|\text{Line1}} =$ | $-90°$ | $90°$ |
| $\phi_{C\|\text{Line2}} =$ | $90°$ | $-90°$ |
| $\phi_{C\|\text{Line3}} =$ | $-90°$ | $-90°$ |

This would result in the following simultaneous ideal $S$ parameter matrices (Equation (1)).

$$[S]|_{f1} = \frac{-j}{\sqrt{2}} \begin{pmatrix} 0 & 1 & 0 & 1 \\ 1 & 0 & 1 & 0 \\ 0 & 1 & 0 & -1 \\ 1 & 0 & -1 & 0 \end{pmatrix} \quad [S]|_{f2} = \frac{-j}{\sqrt{2}} \begin{pmatrix} 0 & -1 & 0 & 1 \\ -1 & 0 & 1 & 0 \\ 0 & 1 & 0 & 1 \\ 1 & 0 & 1 & 0 \end{pmatrix} \quad (1)$$

It can be seen that a signal incoming from Port 1 at frequency $f_1$ evenly splits into two in-phase signals at Ports 2 and 4, whilst at frequency $f_2$ two 180° out of phase signals appear at Ports 2 and 4.

## 3. ARBITRARY PHASE CRLH LINES

### 3.1. Arbitrary Phase CRLH Lines Design

It has to be emphasized that the CRLH lines must show different phase delays at different frequencies. In this case, three different TLs have

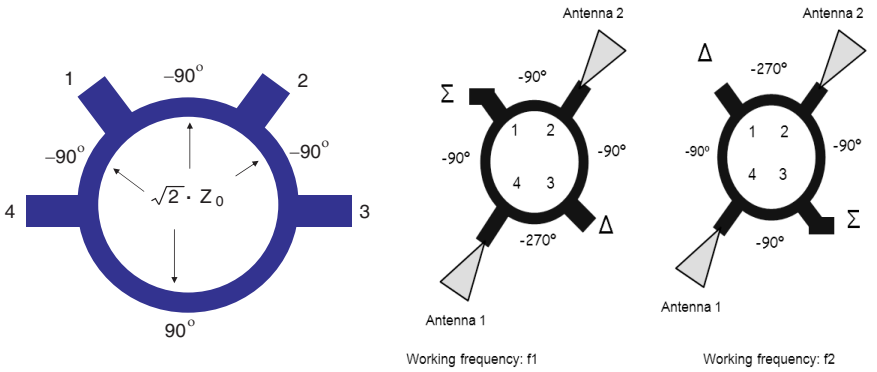


(a) (b)

**Figure 1.** Options for race hybrid. (a) Schematic of a conventional rat-race hybrid. (b) Set up for two dual rat-race couplers with the necessary electric length for the lines.

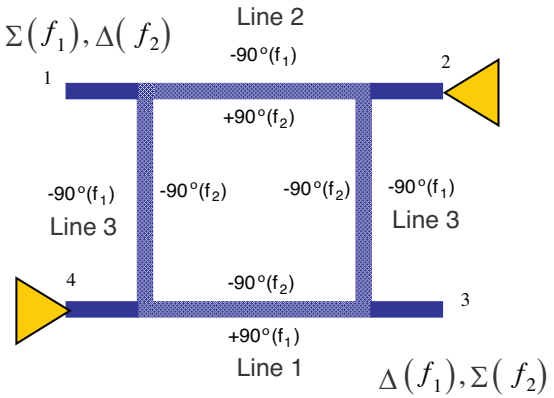


**Figure 2.** Diversity monopulse antenna with a DBDMRR coupler. The inner legend shows the rat-race at one frequency while the outer one shows the other frequency.

to be designed as shown in Table 1. These CRLH lines are composed of conventional RH transmission lines and artificial LH transmission lines. The original LH cell is composed of a series capacitance ($C_L$) plus a shunt inductance ($L_L$). The inductive parasitic component ($L_R$) of the series capacitance and the capacitive parasitic component ($C_R$) of the shunt inductance make impossible the existence of ideal LH lines but composite CRLH lines [3]. For the balanced case, in which the characteristic impedance of the RH and LH TLs are equal, the cells

can be re-arranged, allowing grouping of the RH TLs and the LH cells. The equivalent unit cell of the CRLH TL can be seen in Figure 3(a). The RH TL will be implemented by using microstrip lines. Different technologies have been applied to implement LH TLs: lumped elements (LE), interdigital capacitors and high impedance short stubs or double layer technology.

The phase response of both RH and LH TLs is given by (2). Thus, the phase response of the ideal CRLH is the superposition of phase responses of an ideal LH TL and an ideal RH TL. It then follows that

$$\begin{aligned} \phi_{\mathrm{RH}} &= -N \cdot 2\pi \cdot f\sqrt{L_R \cdot C_R} \\ \phi_{\mathrm{LH}} &= \frac{N}{2\pi \cdot f\sqrt{L_L \cdot C_L}} \\ \phi_C &= \phi_{\mathrm{RH}} + \phi_{\mathrm{LH}} \end{aligned} \tag{2}$$

where $f$ is the frequency, $N$ is the number of cells, $L_L$, $C_L$, $L_R$ and $C_R$ are the LH and RH equivalent lumped elements. At low frequencies, the CRLH TL phase approaches the LH TL phases curve while, at high frequencies, the CRLH TL phase approaches to the RH TL phase curve. As a consequence, the CRLH TL crosses the zero phase axis and the phase slope is the only parameter that can be controlled to achieve the desired phase value shown in Table 1.

This effect can be seen in Figure 3(b) for frequencies of 950 MHz/1.8 GHz. To get the two desired phase delays at the two

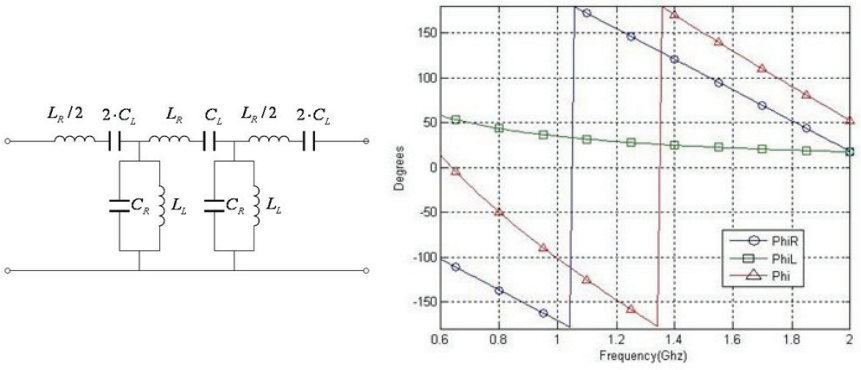


**Figure 3.** CRLH and phase response. (a) Connection of T-type unit cells for artificial CRLH lines. (b) Phase response of the RH, LH and CRLH transmission lines at $f_1$ and $f_2$.

operating frequencies, we can solve the following Equation (3):

$$\begin{aligned} -Pf_1 \ + \ \frac{Q}{f_1} &= \phi_C(f_1) \\ -Pf_2 \ + \ \frac{Q}{f_2} &= \phi_C(f_2) \end{aligned} \tag{3}$$

where:

$$\begin{aligned} P &= 2\pi \cdot N\sqrt{L_R \cdot C_R} \\ Q &= \frac{N}{2\pi\sqrt{L_L \cdot C_L}} \end{aligned} \tag{4}$$

If (3) is solved for the values in Table 1, it follows that:

$$P_1 = \frac{\pi}{2} \cdot \frac{3f_2 - f_1}{f_2^2 - f_1^2} \tag{5}$$

$$Q_1 = \frac{\pi}{2} \cdot \frac{(3f_1 - f_2) \cdot f_1 \cdot f_2}{f_2^2 - f_1^2} \tag{6}$$

$$P_2 = \frac{\pi}{2} \cdot \frac{1}{f_2 - f_1} \tag{7}$$

$$Q_2 = \frac{\pi}{2} \cdot \frac{f_1 \cdot f_2}{f_2 - f_1} \tag{8}$$

$$P_3 = \frac{\pi}{2} \cdot \frac{5f_2 - f_1}{f_2^2 - f_1^2} \tag{9}$$

$$Q_3 = \frac{\pi}{2} \cdot \frac{(5f_1 - f_2) \cdot f_1 \cdot f_2}{f_2^2 - f_1^2} \tag{10}$$

From the previous expressions we can obtain the values of the inductors and capacitors for the LH TL, and with the formulae for a conventional TL (i.e., microstrip) we can design the RH TLs. The characteristic impedance of the CRLH TL must be $\sqrt{2}Z_o$. It is important to highlight that as $f_1$ and $f_2$ get closer, the number of cells in the CRLH line rises. This limits the minimum separation between the frequencies because of practical implementation.

### 3.2. Implementation Technology

All circuits have been fabricated on an Arlon1000 substrate with a dielectric constant of 10 and a thickness of 1.27 mm. The RH TLs are implemented using microstrip lines. The LH TLs are made with

lumped components (inductors and capacitors). The surface-mount-technology (SMT) chip components are 0402 metric. This format has been chosen since the parasitic effects are lower. Their values are shown in Table 2. The capacitors are from Murata and their tolerance is $\pm 0.25$ pF. The inductors are from Coilcraft and have a 2% tolerance. It must be emphasized that as the capacitor values become smaller and smaller the error due to the tolerance becomes more critical.

**Table 2.** Values of the components of the transmission lines.

| Line | $N$, cells | $C_L$ (pF) | | $L_L$ (nH) | | Length |
|---|---|---|---|---|---|---|
| | | Designed | Available | Des. | Av. | RH, mm |
| 1 | 2 | 3.7 | $4.0\,(2 \times 2.0)$ | 19 | 22 | 53.6 |
| 2 | 3 | 2.1 | $2.2\,(1.2 + 2)$ | 11 | 11 | 32.4 |
| 3 | 3 | 2.0 | $2.0\,(2 \times 1.0)$ | 10 | 11 | 98.8 |

The two operating frequencies have been chosen as 950 and 1800 MHz (in the GSM band) resulting in a frequency ratio of 1.9. The three transmission lines have been simulated with Microwave Office (AWR®). Figure 4 and Figure 5 show the simulated and measured parameters for the designed CRLH lines. The transmission parameter for the three lines is lower than 0.5 dB except at higher frequencies where the amplitude imbalance is larger. This may be due to the capacitor tolerance which is more critical at higher frequencies. The phase response of the lines is within a maximum error of 3 degrees from the desired response at the two frequencies. It can also be noticed that there is a shift in the higher frequency.

The main advantages of the surface-mount-technology are its simplicity and availability. However, one of the most important problems arises from the high tolerance of the capacitors. This is particularly critical when the capacitor values must be accurate. It must also be noted that not all the designed values are available. In addition, when the number of CRLH sections rises (i.e., when the frequency separation gets closer) the number of soldering points increases and the parasitic effects associated to the lines enlarge. Thus, for the constructed lines, the capacitor tolerance varies between 5% for the 4.7 pF case up to 25% for the 1 pF case. This has been taken into account in the hybrid design.

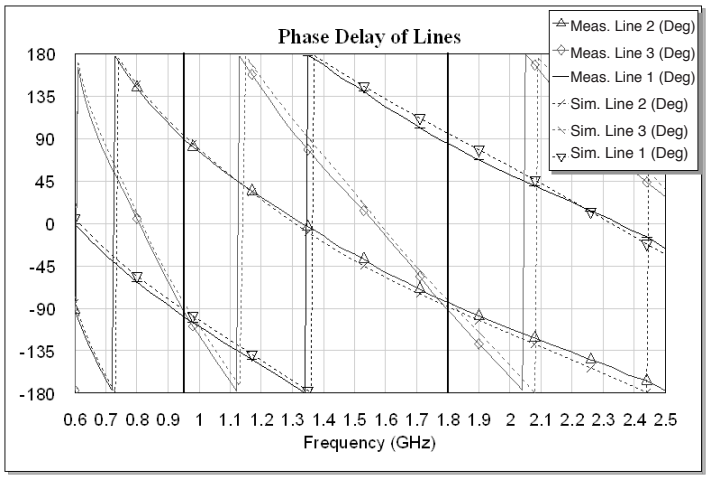


**Figure 4.** Simulated and measured phase delay in the three CRLH TL designed.

## 4. DUAL-BAND DUAL-MODE RAT-RACE COUPLER: SIMULATIONS AND MEASUREMENTS

A dual frequency dual-mode rat-race coupler has been built and measured. Figure 6 shows the photograph of the prototype.

Simulation and measurements of this device show good agreement. The upper band has slightly shifted from 1800 MHz to 1740 MHz. The DBDMRR is matched at the two working frequencies, with return losses of 24 dB and 33 dB, respectively for the lower and higher cases. In the two passbands, the transmission parameters $s_{21}$ and $s_{41}$ are very close to the simulated values. The difference between Ports 2 and 4 is only 0.8 dB in both bands. The isolation between ports is not as good as simulated, resulting in only 25 dB.

Concerning the phase response, Figure 11 shows the phase difference between the output ports. It can be seen that at $f_1$ two ports are in phase and the other two ports are 180° out of phase, whereas at the other frequency, the situation is changed. The phase difference error is lower than 3° at the frequencies considered.

Finally all the performances in both bands are summarized in Table 3 and Table 4.

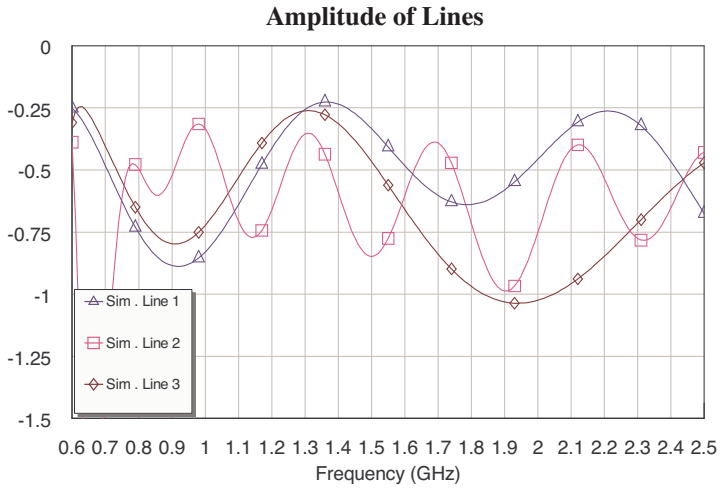


(a)

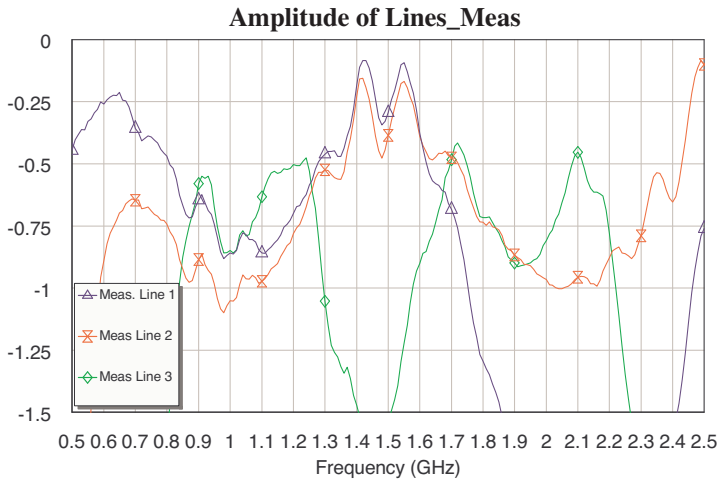


(b)

**Figure 5.** Simulated and measured transmission parameter for the three CRLH TLs.

## 5. DIVERSITY MONOPULSE ANTENNA

The monopulse antenna is composed of two low profile broadband commercial monopoles that have been externally matched to cover the two working frequencies of the DBDMRR. Two identical antennas are set at Ports 2 and 4 according to Figure 2.

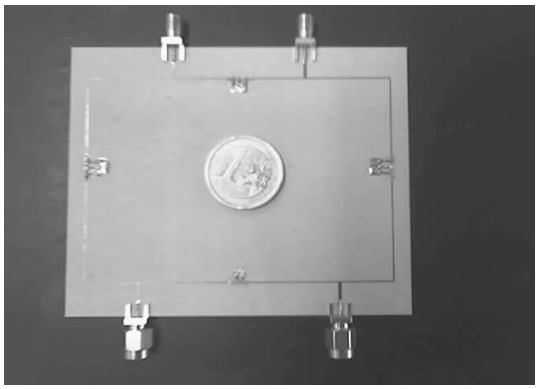

**Figure 6.** Photograph of the complete DBDMRR.

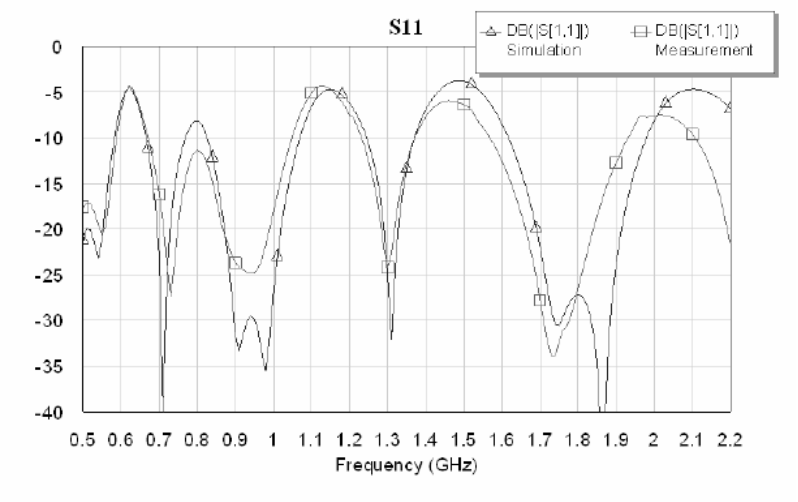


**Figure 7.** Simulated and measured return losses for the DBDMRR.

The monopole antenna is a truncated rhombus with an external resistive load to enlarge the impedance bandwidth and cover the two working frequencies. The setup of the monopulse antenna is illustrated in Figure 12. Both antennas are connected to the DBDMRR input ports. The schematic in Figure 12 also shows the $E$ plane and the $H$ plane. The $\Sigma$ and $\Delta$ radiation patterns in the $H$ plane will be considered below.

The radiation patterns of the previous antenna have been measured and are presented in Figure 13 and Figure 14. Figure 13

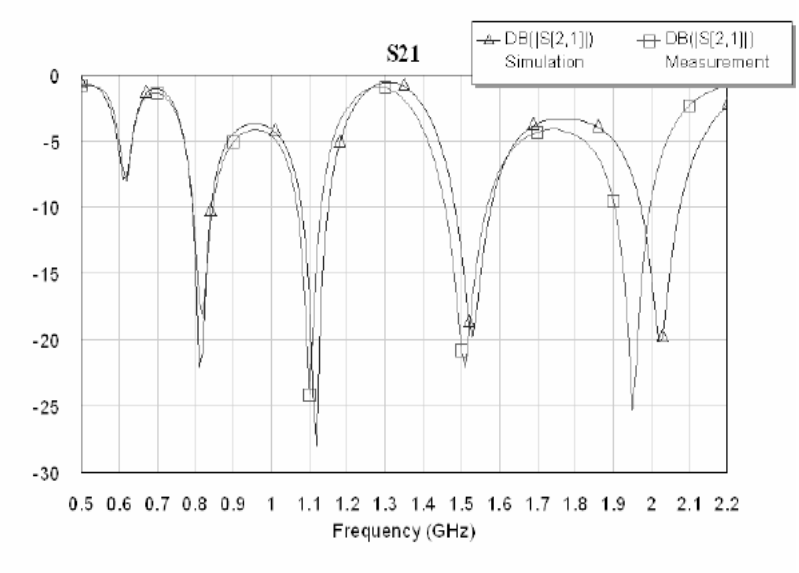


**Figure 8.** Simulated and measured transmission parameter ($s_{21}$) for the DBDMRR ($\Delta$ simulated and $\square$ measured).

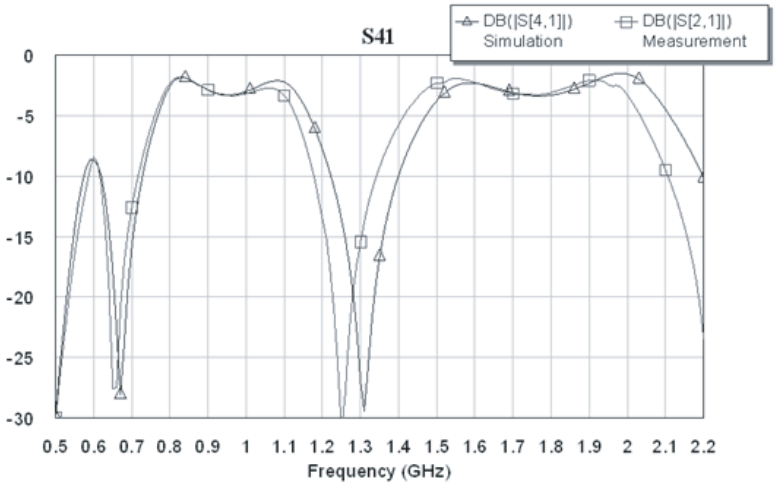


**Figure 9.** Simulated and measured coupling parameter ($s_{41}$) for the DBDMRR ($\Delta$ simulated and $\square$ measured).

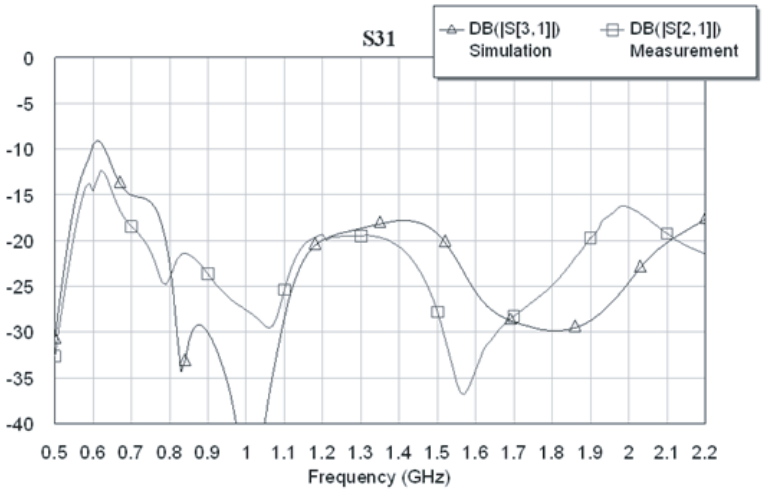


**Figure 10.** Simulated and measured isolation ($s_{31}$) for the DBDMRR ($\Delta$ simulated and $\square$ measured).

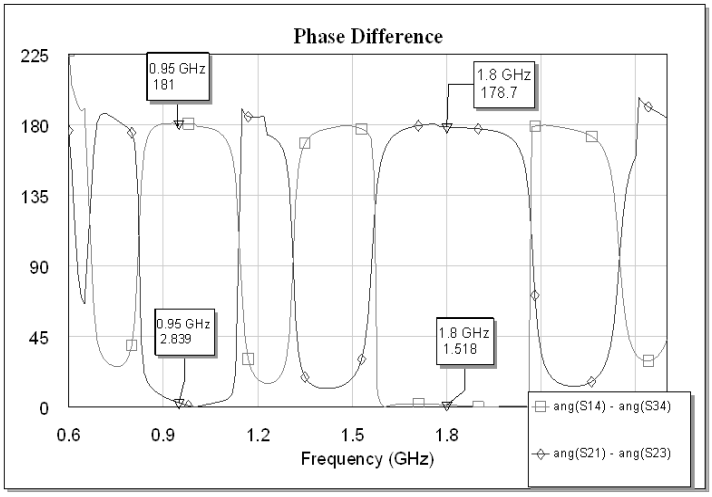


**Figure 11.** Phase difference between outputs of the DBDMRR.

shows the copolar and crosspolar components at the $E$-plane. It can be seen that there is a small error in the pointing direction (towards $-5^\circ$ instead of $0^\circ$) that could be due to the finite ground plane or to the fact that the phase difference at the two working frequencies of the DBDMRR is not exactly the same at the two ports and somewhat

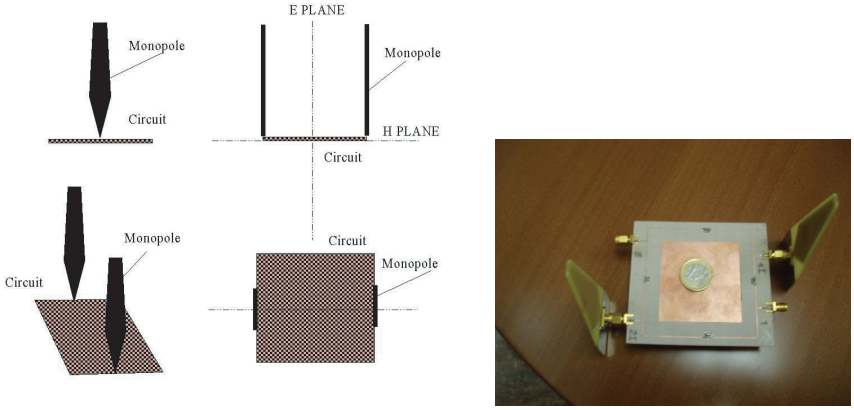


(a) Schematic (b) Photograph

**Figure 12.** Schematic and photograph of the monopulse antenna.

**Table 3.** Performance of the device in the first passband.

| | **Simulation** | **Measurement** |
|---|---|---|
| Frequency ($f_1$) | 0.95 GHz | 0.96 GHz |
| Return Loss ($s_{11}$) | −29.9 dB | −24.3 dB |
| Isolation ($s_{31}$) | −35.4 dB | −26.4 dB |
| Output 1 ($s_{21}$) | −3.7 dB | −4.1 dB |
| Output 2 ($s_{41}$) | −3.3 dB | −3.4 dB |
| Amp. Imbalance | 0.4 dB | 0.7 dB |
| Phase Difference | 2.9° | 3.3° |
| BW 1 dB | 80 MHz (8.4%) | 50 MHz (5.3%) |

different from 180°. The previous error is a little larger at the higher frequency. It can also be seen that the ratio between co-polar and cross-polar components is larger than 35 dB at the two working frequencies at the pointing direction.

The performance of the monopulse antenna is seen in the $H$-plane radiation patterns. According to Figure 2, at the lower frequency, 950 MHz ($f_1$), the output ports (1 and 3) are the $\Sigma$ and the $\Delta$ cases respectively. However, the performance at the upper frequency, 1740 MHz ($f_2$), is different since the output ports have been changed. Then, Port 1 is the $\Delta$ one, while Port 3 is the $\Sigma$ case. These patterns are seen in Figure 14. The error in the pointing direction causes both,

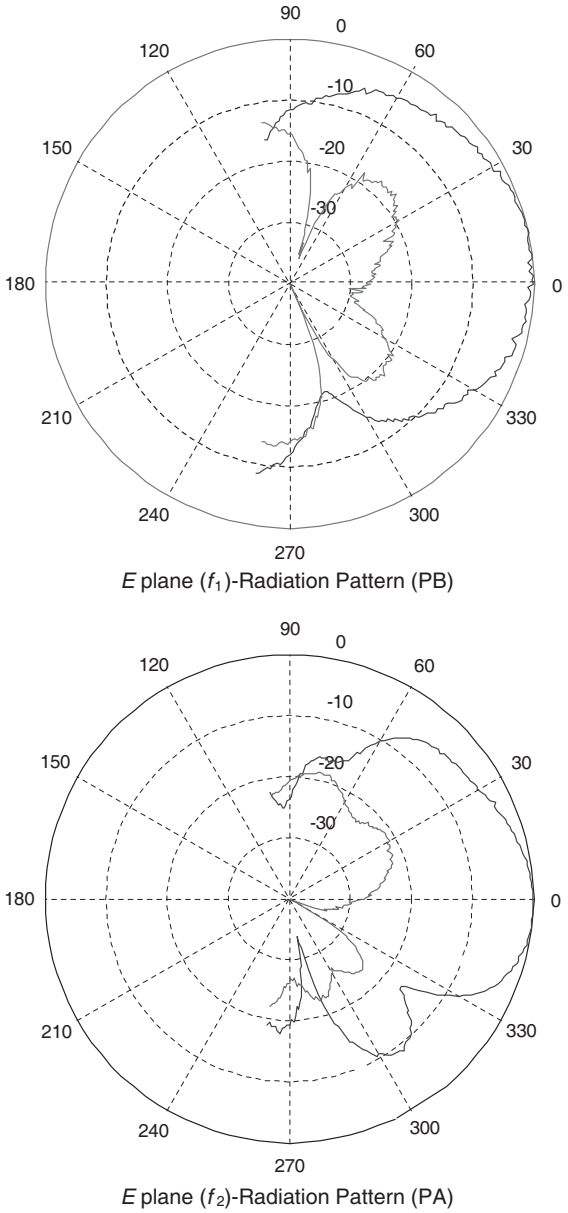


**Figure 13.** Polar $E$-plane radiation patterns of the two element array antenna at the two working frequencies of the DBDMRR.

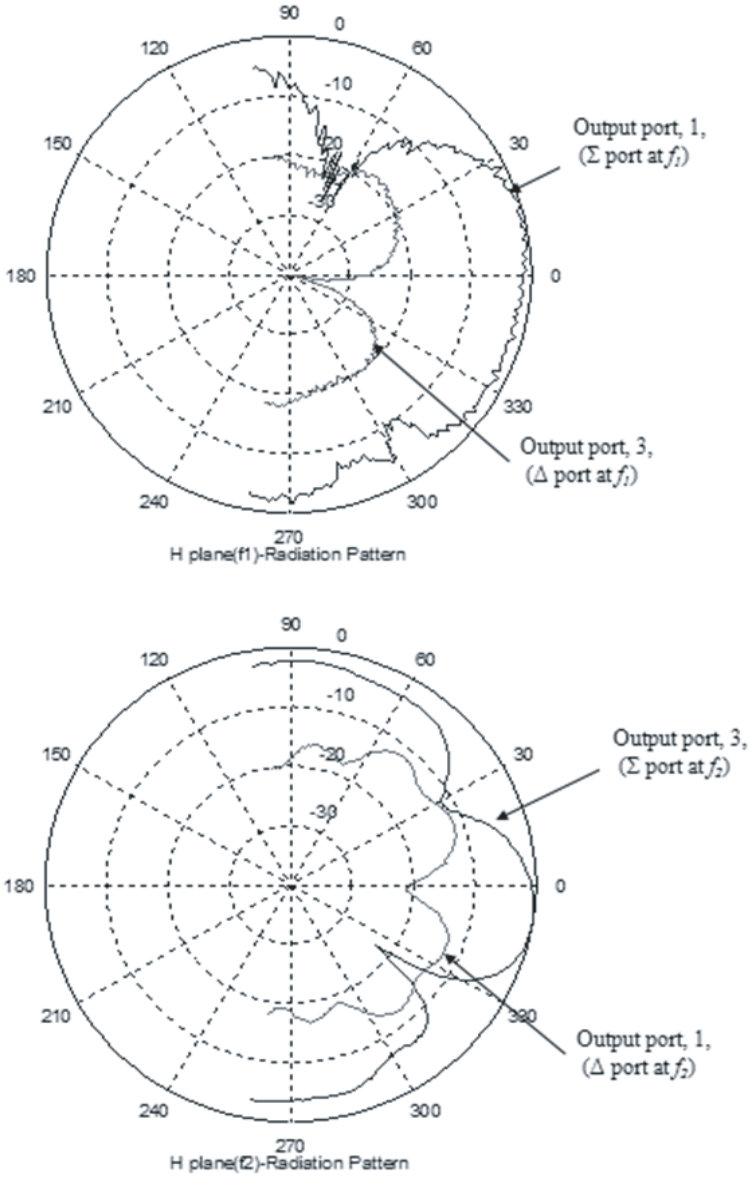


**Figure 14.** $H$-plane radiation patterns of the monopulse antenna at the two working frequencies of the DBDMRR.

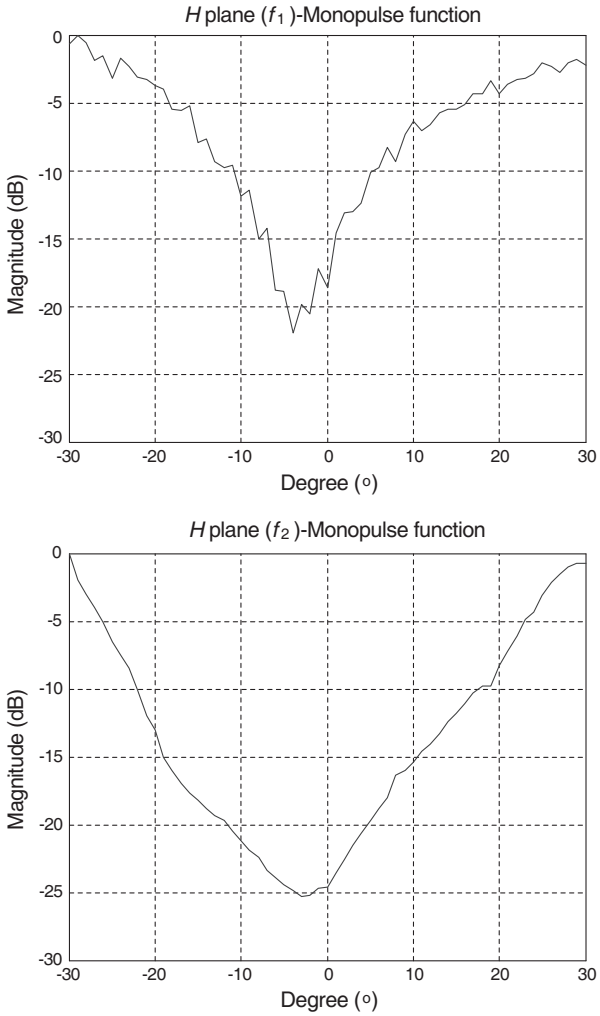


**Figure 15.** Ratio of the difference ($\Delta$) and sum ($\Sigma$) patterns at the two working frequency.

the $\Sigma$ and $\Delta$ patterns, to have an offset of $-5^\circ$ respect the desired pointing direction. The cause of this mispointing error is associated to the finite size of the ground plane.

In addition, as the DBDMRR has diplexing properties, two monopulse processors can be directly connected at both ports to determine the angle of arrival at either frequency. In this way, a diplexer to separate the $\Sigma$ or $\Delta$ outputs is avoided. Thus, the

**Table 4.** Performance of the device in the second passband

| | **Simulation** | **Measurement** |
|---|---|---|
| Frequency ($f_2$) | 1.77 GHz | 1.75 GHz |
| Return Loss ($s_{11}$) | −28.7 dB | −32.3 dB |
| Isolation ($s_{31}$) | −29.7 dB | −27 dB |
| Output 1 ($s_{21}$) | −3.3 dB | −4.0 dB |
| Output 2 ($s_{41}$) | −3.4 dB | −3.3 dB |
| Amp. Imbalance | 0.1 dB | 0.7 dB |
| Phase Difference | 177.9° | 173.9° |
| BW 1 dB | 170 MHz (9.6%) | 60 MHz (3.4%) |

monopulse processor can be connected to obtain the monopulse function: ratio of difference ($\Delta$) and sum ($\Sigma$) patterns. It may be seen that there are two deep unambiguous nulls at either frequency capable of high resolution. The null of the monopulse function is deeper than 20 dB at either of the two working frequencies. As it was expected, it must also be noticed that the slope at higher frequency is sharper than at the lower one. Figure 15 shows the ratio of the difference and sum patterns at the two working frequencies.

## 6. CONCLUSION

A diversity monopulse antenna based on a dual-band dual-mode CRLH rat-race coupler has been presented in this paper. This topology requires dual frequency TL with opposite phase delay to be used in order to avoid later diplexers. The only way of designing these transmission lines with opposite phase delays is by using lines based on metamaterial structures. CRLH lines have been used to achieve that goal. The CRLH DBDMRR has been designed and built at 950 MHz/1800 MHz. Excellent agreement has been obtained between measurements and simulation. Return losses larger than 24 dB have been obtained in both bands. Transmission and coupling parameters are around 3.6 dB. Isolation larger than 25 dB has been achieved. A little displacement in the upper frequency has happened. Finally, the monopulse antenna has been built and measured showing the $\Sigma$ and $\Delta$ radiation patterns at alternate ports at the two working frequencies.

## ACKNOWLEDGMENT

The authors want to thank J.M Gómez-Pulido for his help in the radiation pattern measurements and Dr. Carlos Martín-Pascual and Dr. José Luis Jiménez for his helpful comments in the discussion about the paper. This work was supported by the Spanish Ministry of Science and Technology under project TEC2006-13248-C04-04.

## REFERENCES

1. Harabi, F., H. Changuel, and A. Gharsallah, "Direction of arrival estimation method using a 2-L shape arrays antenna," *Progress In Electromagnetics Research*, PIER 69, 145–160, 2007.
2. Lipsky, S. E., "Microwave passive direction finding," *Wiley Interscience*, 1987.
3. Song, M. Z. and T. Hong, "Sum and difference multiple beam modulation transmitted by multimode horn antenna for inverse monopulse direction finding," *Progress In Electromagnetics Research*, PIER 82, 367–382, 2008.
4. Lee, K. C., C.W. Huang, and M.C. Fang, "Radar target recognition by projected features of frequency-diversity RCS," *Progress In Electromagnetics Research*, PIER 81, 121–133, 2008.
5. Lin, I.-H., M. de Vicentis, C. Caloz, and T. Itoh, "Arbitrary dual-band components using composite right/left-handed transmission lines," *IEEE Trans. on Microwave Theory and Techniques*, Vol. 52, No. 4, 1142–1149, April 2004.
6. Keung, K. and M. Cheng, "A novel approach to the design and implementation of dual-band compact planar 90 branch-line coupler," *IEEE Trans. on Microwave Theory and Techniques*, Vol. 52, No. 11, November 2004.
7. Niu, J. X. and X. L. Zhou, "Analysis of balanced composite right/left handed structure based on different dimensions of complementary split ring resonators," *Progress In Electromagnetics Research*, PIER 74, 341–351, 2007.
8. Smith, D. R., W. J. Padilla, D. C. Vier, S. C. Nemat Nasser, and S. Schultz, "Composite medium with simultaneous negative permeability and permittivity," *Physical Review Letters*, Vol. 84, No. 18, 4184–4187, May 2000.
9. Caloz, C. and T. Itoh, "Novel microwave devices and structures based on the transmission line approach of meta-materials," *IEEE MTT-S Int. Microwave Symp. Dig.*, Vol. 1, 195–198, June 2003.
10. Iyer, K. and G. V. Eleftheriades, "Negative refractive-index meta-

materials supporting 2-D waves," *IEEE MTT-S Int. Microwave Symp. Dig.*, Vol. 2, 1067–1070, Seattle, WA, June 2002.

11. Engheta, N. and R. W. Ziolkowski, "AA positive future for double negative metamaterials," *IEEE Trans. on Microwave Theory and Techniques*, Vol. 53, No. 4, Special Issue on Metamaterials, Part II, 1535–1556, April 2005.
12. Caloz, C. and T. Itoh, "Transmission line approach for left-handed (LH) materials and microstrip implementation of an artificial LH transmission line," *IEEE Trans. on Antennas and Propagation*, Vol. 52, No. 5, 1159–1166, May 2004.
13. Okabe, H., C. Caloz, and T. Itoh, "A compact enhanced-bandwidth hybrid ring using an artificial lumped-element left-handed transmission-line section," *IEEE Trans. on Microwave Theory and Techniques*, Vol. 52, No. 3, 798–804, March 2004.
14. Caloz, C., A. Sanada, and T. Itoh, "A novel composite right-/left-handed coupled-line directional coupler with arbitrary coupling level and broad bandwidth," *IEEE Trans. on Microwave Theory and Techniques*, Vol. 52, No. 3, 980–992, March 2004.
15. Ziolkowski, R. W. and A. Kipple, "Application of double negative metamaterials to increase the power radiated by electrically small antennas," *IEEE Trans. on Antennas and Propagation*, Vol. 51, No. 10, 2626–2640, October 2003.
16. Sanada, A., M. Kimura, I. Awaii, H. Kubo, C. Caloz, and T. Itoh, "A planar zeroth-order resonator antenna using left-handed transmission line," *Proc. of the 34th European Microwave Conference*, 1341–1344, Amsterdam, October 2004.
17. Yu, A., F. Yang, and A. Z. Elsherbeni, "A dual band circularly polarized ring antenna based on composite right and left handed metamaterials," *Progress In Electromagnetics Research*, PIER 78, 73–81, 2008.
18. Castro-Galan, D., V. Gonzalez-Posadas, C. Martin-Pascual, and D. Segovia-Vargas, "Novel diplexer based on CRLH transmission lines," *Proc. of the 35th European Microwave Conference*, Paris, October 2005.